Molecular Physics

An International Journal at the Interface Between Chemistry and Physics

ISSN: (Print) (Online) Journal homepage: https://www.tandfonline.com/loi/tmph20

An *ab initio* journey into the electronic structure of Be_3

Apostolos Kalemos

To cite this article: Apostolos Kalemos (26 Dec 2023): An *ab initio* journey into the electronic structure of Be_3, Molecular Physics, DOI: 10.1080/00268976.2023.2297822

To link to this article: https://doi.org/10.1080/00268976.2023.2297822

MOLECULAR PHYSICS e2297822
https://doi.org/10.1080/00268976.2023.2297822

Taylor & Francis
Taylor & Francis Group

RESEARCH ARTICLE

An *ab initio* journey into the electronic structure of Be_3

Apostolos Kalemos

Department of Chemistry, Laboratory of Physical Chemistry, National and Kapodistrian University of Athens, Athens, Hellas

ABSTRACT

In the present study, we concisely report on Be_3's ground and several excited states of singlet, triplet, quintet, and septet spin symmetry at the MRCI/aug−cc−pV5Z computational level. We have constructed potential energy cuts along the bending coordinate under both C_{2v} and C_s symmetry constraints. Both linear and bent configurations have been calculated that span an energy range of nearly 160 kcal/mol. The excited states result by promoting one, two or three valence electrons from the ground state's electronic configuration. This electronic promotion destroys its sigma (2center – $2e^-$) bond(s) and the resulting asymmetry is at the very heart of the Jahn–Teller distortion.

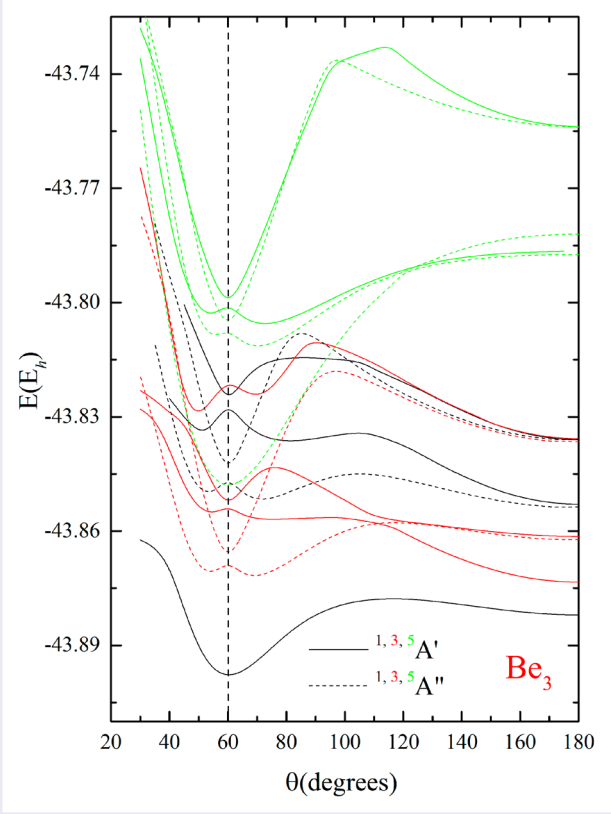

ARTICLE HISTORY
Received 11 November 2023
Accepted 18 December 2023

KEYWORDS
Berylium clusters; Non adiabatic coupling elements; chemical bond

1. Introduction

Despite the 'innocent' rare gas $1s^2 2s^2$ electronic configuration of the ground (^{1}S) state Be atom, it is an element of intrinsic complexity [1, 2]. Its dimer, Be_2, is a covalently bonded system (see *e.g.* Refs. [3, 4]) with a very small adiabatic binding energy (D_e (exp) = 934.9 ± 0.4 cm^{-1}, r_e (exp) = 2.445(5) Å, Ref. [5]) while its chemical bonding puzzled the scientific community for nearly 60 years.

CONTACT Apostolos Kalemos kalemos@chem.uoa.gr Department of Chemistry, Laboratory of Physical Chemistry, National and Kapodistrian University of Athens, Athens 157 71, Hellas

Despite the above peculiar characteristics, beryllium is a highly toxic metal with a melting point at about 1300 °C [6].

It seems that its first theoretical description is a 1975 study by Bulski who studied the three-body contributions to the exchange repulsion [7]. At the *ab initio* level its first post-HF study appears to be the MRCI/[7*s*4*p*2*d*] calculations by Harrison and Handy [8] who in 1986 predicted a binding energy of 19(21) kcal/mol at the CI(+Q) level. Some years later, Lee, Rendell, and Taylor [9] calculated Be and Mg clusters with a variety of computational methods. Their best results for Be_3 are $r_e = 4.199$ bohr and $D_e = 22.4$ kcal/mol at the MRCI(0.025)/[5321] level while their best estimate for the binding energy is 24 kcal/mol. In 2000, Kaplan, Roszak, and Leszczynski [10] studied the nature of the bonding in Be_3, Mg_3, and Ca_3 and concluded that it is due to two body localised dispersion forces and three body delocalised exchange forces. In a FCI/[3*s*2*p*1*d*] study by Junquera-Hernández *et al.* [11] a $D_e = 17.2$ kcal/mol is reported for its most stable D_{3h} configuration. The same authors reported a similar FCI/[3*s*2*p*1*d*] study for several vertical singlet excited states [12]. An AQCC calculation based on a large CASSCF reference wavefunction gave a $D_e = 27.3$ kcal/mol (aug–cc–pV5Z) at $r_e = 4.101$ bohr (cc–pV5Z) [13]. The authors also performed an EPFL analysis that showed the crucial role of the 2*p* orbitals in the formation of the chemical bond. By a similar computational strategy (CASSCF + AQCC) Ramírez-Solís and Novaro [14] attributed the large binding energy of the trimer (26.1 kcal/mol) to non-additive collective effects that amount to nearly 94% of the D_e.

The experimental and theoretical corpus on Be clusters has been recently reviewed in [15] and [16], while the latest experimental work [17] on Be_3 and Be_4 proves the enormous academic interest on its chemistry.

We have gained considerable experience on Be bonding through our recent studies on different species such as Be_2 [3], beryllium oxides [18], BeF^- [19], Be_3^- [20], and finally BeH^- [4]. A common trait in all of the above species is the participation of the excited $2s^1 2p^1$ configuration ($\Delta E(^3P \leftarrow {}^1S) = 2.725$ eV and $\Delta E(^1P \leftarrow {}^1S) = 5.277$ eV, Ref. [21]) in the formation of both covalent and dative bonds; see *e.g.* Ref. [4] for an adiabatic to diabatic transformation that explicitly shows the presence of the excited $2s^1 2p^1$ configuration in the bonding process.

We have studied Be_3's ground state in Ref. [3] and its anion, Be_3^-, in Ref. [20]. In the latter study, eleven electronic states have been detailed that were associated to five states of its parental neutral species. Its ground state is of equilateral geometry (D_{3h}) and of $\tilde{X}^1A'_1$ symmetry. Its bonding results when three excited ^3P Be atoms form sigma (type) bonds with each other. The ground anionic state results when an additional electron is drafted to the π system ($^2B_1$) of the neutral species (EA = 1.379 eV, [20]) while its first excited state results when the minus charge resides in the molecular plane ($^2A_1$, ΔE ($^2A_1 \leftarrow {}^2B_1$) = 0.359 eV). In our present study we focus exclusively on the neutral Be_3 system with the aim to delve more deeply into its electronic structure by elucidating as many states as possible.

2. Computational details

Beryllium trimer is a six-electron valence system that can form states of singlet, triplet, quintet, and septet spin multiplicity. We have constructed potential energy profiles along the bending coordinate for the low-lying states of each space–spin symmetry by optimising a C_{2v} geometry under both C_{2v} and C_s symmetry constraints. Our zeroth-order wavefunction is of the complete active space self-consistent field (CASSCF) type whose active space is composed of 12 valence orbitals converging at infinity to the atomic 2*s* and 2*p* Be orbitals. Additional dynamic correlation was extracted through the internally contracted multi-reference configuration interaction (MRCI) method built upon the CASSCF reference. The aug − cc − pV5Z basis set [22] was employed and the MOLPRO computational package [23] was used.

3. Results and discussion

A panoramic view of the calculated states is displayed in Figure 1 while numerical results are gathered in Table 1. In Figure 1 we show potential energy cuts along the bending coordinate when a C_{2v} geometry is optimised under C_{2v} symmetry constraints. Different spin multiplicities are displayed in different colour; black for singlets, red for triplets, green for quintets, and blue for septets while solid lines are used for energy profiles that transform as A′ under C_s symmetry constraints and dashed lines for those states that transform as A″. Only the lowest energy states of each space–spin symmetry label have been calculated at the MRCI computational level. A vertical line at 60 degrees highlights the symmetry imposed conical intersections of Jahn–Teller (JT) character. For selected (space–spin) states we have also calculated the energy cuts at C_s symmetry constraints (see Figure 2). The latter C_s profiles are more appropriate for the study of nuclear dynamics although the crossing ones (C_{2v}) turn out to be more easily manipulated when no adiabatic effects are in order.

The Be_3 ground state is of D_{3h} geometry and $^1A_1$ (C_{2v}) symmetry and it results from the interaction of three excited Be atoms that form 2c(enter) – $2e^-$ bonds with their adjacent atoms (see Refs. [3] and [4]).

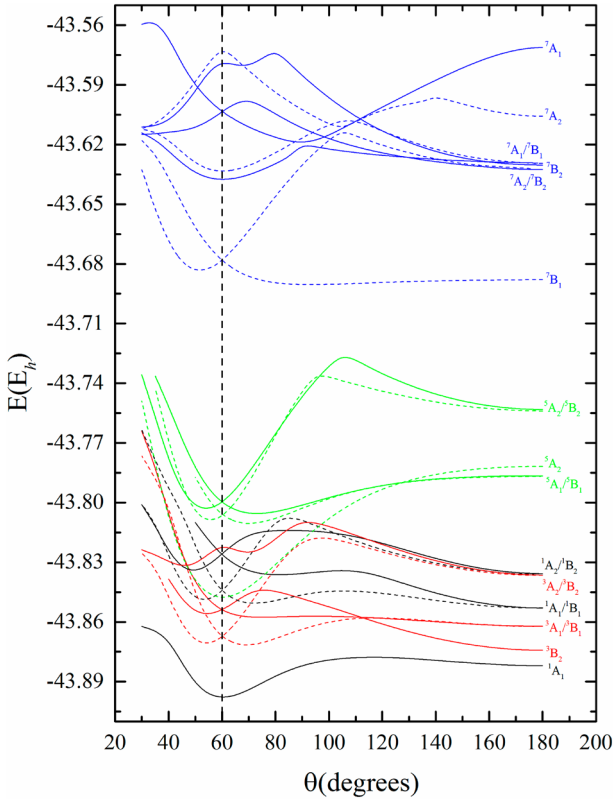

Figure 1. MRCI/aug − cc − pV5Z potential energy profiles of Be_3 states of singlet (black), triplet (red), quintet (green), and septet (blue) spin symmetry along the bending coordinate under C_{2v} symmetry constraints. Solid lines are used for energy profiles that transform as A′ under C_s symmetry constraints and dashed lines for those states that transform as A″.

The excited nature of the atomic constituents is also revealed by the calculation of the non adiabatic coupling matrix elements (NACME) along the asymmetric dissociation path $Be_3 \rightarrow Be_2 + Be$ (see Figure 3). Its ground state dissociates adiabatically to ground state fragments, *i.e.* Be_2 $(X^1\Sigma_g^+) + Be$ (^1S). But around its equilibrium configuration, there are intense NACMEs with the 2nd and 3rd $^1A'$ states that converge asymptotically to 3 $^1\Pi_g + {}^1S$ and 6 $^1\Pi_u + {}^1S$, respectively. The latter Be_2 molecular states result from the combination of Be $(^1S) + Be\,(^1P)$ [3]. So due to the centrosymmetric character of the diatomic and the C_3 symmetry of the triatomic the excited $2s^12p^1$ nature of the atomic centers in Be_3 occurs naturally. The ground state is bound by 24.5(25.5) kcal/mol at the MRCI(+Q) computational level with respect to three Be (^1S) atoms at $r_e = 2.203$ Å. Our numerical data compare well with the previous reported values of 24 ($r_e = 2.222$ Å) [9], 27.3 ($r_e = 2.170$ Å) [13], and 26.1 kcal/mol ($r_e = 2.170$ Å) [14].

A vertical excitation from the ground state ends up to the conical intersection of two curves of $^3B_1$ and $^3A_2$ symmetry (see Figure 1) that under C_s transform into a double minimum $^3A''$ curve and another $^3A''$ curve whose minimum sits on the energy maximum of its JT companion (see Figure 2). On the lowest $^3A''$ curve the minimum at 68.7° (see Table 1) is of $^3B_1$ symmetry and correlates to a $^3\Pi_u$ linear configuration while the minimum at 53.9° is of $^3A_2$ symmetry and correlates to a linear $^3\Pi_g$ state. It is interesting to observe the equilibrium configurations of these two triplet states and compare them to those of its ground state:

$$|\tilde{X}^1A_1\rangle \cong 0.87|1a_1^2 2a_1^2 1b_2^2\rangle,$$
$$|4^3B_1\rangle \cong 0.90|1a_1^2 2a_1^1 1b_1^1 1b_2^2\rangle - 0.20|1a_1^2 2a_1^1 3a_1^2 1b_1^1\rangle - 0.11|1a_1^2 2a_1^1 1b_1^1 2b_2^2\rangle, \quad \text{and}$$
$$|5^3A_2\rangle \cong 0.89|1a_1^2 2a_1^2 1b_1^1 1b_2^1\rangle - 0.22|1a_1^2 3a_1^2 1b_1^1 1b_2^1\rangle.$$

The triplet states result from the excitation of a $2a_1$ ($\tilde{X}^1A_1 \rightarrow 4\,^3B_1$) or a $1b_2$ ($\tilde{X}^1A_1 \rightarrow 5\,^3A_2$) electron to an orbital of b_1 symmetry (perpendicular to the molecular plane), respectively. The other contributions offer a GVB-type correlation to the $1b_2$ ($4\,^3B_1$) or $2a_1$ ($5\,^3A_2$) electron pairs. In chemical terms one of the 2c – $2e^-$ sigma bonds of the ground state becomes a 2c – $1e^-$ sigma bond and this creates a bonding asymmetry which is the chemical origin of the JT distortion.

The second excited state that can be reached vertically is a manifold of two JT states of (7) $^3A_1$ and (8) $^3B_2$ symmetry. Under C_s symmetry constraints these two crossing curves give rise to two $^3A'$ profiles that correlate to $^3\Sigma_u^+$ and $^3\Pi_u$ linear states, respectively. Once again the lowest $^3A'$ sheet displays two minima of $^3A_1$ (at 73.9°) and $^3B_2$ (at 54.3°) symmetry, respectively. This pair of $^3A'$ states display not only a symmetry imposed conical intersection but also an accidental one at around 112°; see Figures 1 and 2. Once again the equilibrium configurations provide an insight into their bonding situation. These are

$$|7^3A_1\rangle \cong 0.88|1a_1^2 2a_1^1 3a_1^1 1b_2^2\rangle + 0.20|1a_1^2 2a_1^2 1b_2^1 2b_2^1\rangle - 0.16|1a_1^2 2a_1^1 3a_1^2 2b_2^2\rangle - 0.15|1a_1^2 3a_1^2 1b_2^1 2b_2^1\rangle,$$

and

$$|8^3B_2\rangle \cong 0.89|1a_1^2 2a_1^2 3a_1^1 1b_2^1\rangle - 0.20|1a_1^2 3a_1^1 4a_1^2 1b_2^1\rangle.$$

It is evident that the 7 $^3A_1$ state results mainly from the closed shell ground state configuration ($|\tilde{X}^1A_1\rangle \cong 0.87|1a_1^2 2a_1^2 1b_2^2\rangle$) by exciting a $2a_1$ electron to the $3a_1$ orbital while the 8 $^3B_2$ state results when a $1b_2$ electron gets also promoted to the $3a_1$ orbital.

The next state to be considered is of $^5A_2$ ($|12^5A_2\rangle \cong 0.94|1a_1^2 2a_1^1 3a_1^1 1b_1^1 1b_2^1\rangle$) symmetry that relates to a $^5\Sigma_u^-$ linear configuration. It results from the ground state configuration by promoting an electron from $2a_1$ to $3a_1$ and

Table 1. Energies E(hartree), bond distances r_e (Å), bond angles $\theta_{Be_2Be_1Be_3}$ (degrees), energy gaps ΔE (kcal/mol) and main configurations of the Be_3 states presently studied at the MRCI/aug − cc − pV5Z computational level. A C_{2v} notation is used for the bent configurations, r_e refers to the bond length between the middle (Be_1) and the terminal ($Be_{2,3}$) atoms while linear configurations lie on the y axis with Be_1 placed on the origin. At the MRCI/aug − cc − pV5Z level the atomic Be energies are E (^{1}S) = −14.619 196 E_h and E (^{3}P) = −14.518 666 E_h.

State	−E	r_e	$\theta_{Be_2Be_1Be_3}$	ΔE	Main configurations
$\tilde{X}^1A_1$	43.898 160	2.203	60.0	0.0	$\|\tilde{X}^1A_1\rangle \cong 0.87\|1a_1^2 2a_1^2 1b_2^2\rangle$
$2^1\Sigma_g^+$	43.882 018	2.207	180.0	10.1	$\|2^1\Sigma_g^+\rangle \cong \|1a_1^2(0.77 \times 2a_1^2 - 0.53 \times 2b_2^2)1b_2^2\rangle$
$3^3\Sigma_u^+$	43.874 237	2.145	180.0	15.0	$\|3^3\Sigma_u^+\rangle \cong 0.95\|1a_1^2 2a_1^1 1b_2^2 2b_2^1\rangle$
4^3B_1	43.872 020	1.991	68.7	16.4	$\|4^3B_1\rangle \cong \|1a_1^2 2a_1^1 1b_1^1(0.90 \times 1b_2^2 - 0.20 \times 3a_1^2)\rangle$
5^3A_2	43.871 463	2.134	53.9	16.8	$\|5^3A_2\rangle \cong \|1a_1^2(0.89 \times 2a_1^2 - 0.22 \times 3a_1^2)1b_1^1 1b_2^1\rangle$
$6^3\Pi_u$	43.862 156	2.071	180.0	22.6	$\|6^3\Pi_u(^3B_1)\rangle \cong 0.88\|1a_1^2 2a_1^1 1b_1^1 1b_2^2\rangle - 0.22\|1a_1^2 1b_2^2 2b_2^1 1a_2^1\rangle$
7^3A_1	43.858 070	2.079	73.9	25.2	$\|7^3A_1\rangle \cong 0.88\|1a_1^2 2a_1^1 3a_1^1 1b_2^2\rangle$
8^3B_2	43.856 396	2.239	54.3	26.2	$\|8^3B_2\rangle \cong 0.89\|1a_1^2 2a_1^2 3a_1^1 1b_2^1\rangle$
$9^1\Pi_u$	43.853 637	2.054	180.0	27.9	$\|9^1\Pi_u(^1B_1)\rangle \cong 0.85\|1a_1^2 2a_1^1 1\bar{b}_1^1 1b_2^2\rangle - 0.31\|1a_1^2 1b_2^2 2b_2^1 1\bar{a}_2^1\rangle$
10^1B_1	43.851 745	1.987	71.5	29.1	$\|10^1B_1\rangle \cong 0.89\|1a_1^2 2a_1^1 1\bar{b}_1^1 1b_2^2\rangle - 0.18\|1a_1^2 2a_1^1 3a_1^2 1\bar{b}_1^1\rangle$
11^1A_2	43.850 494	2.155	53.1	29.9	$\|11^1A_2\rangle \cong 0.89\|1a_1^2(0.89 \times 2a_1^2 - 0.21 \times 3a_1^2)1b_1^1 1\bar{b}_2^1\rangle$
12^5A_2	43.848 122	1.998	60.0	31.4	$\|12^5A_2\rangle \cong 0.94\|1a_1^2 2a_1^1 3a_1^1 1b_1^1 1b_2^1\rangle$
13^1A_1	43.837 108	2.026	80.8	38.3	$\|13^1A_1\rangle \cong 0.78\|1a_1^2 2a_1^1 3\bar{a}_1^1 1b_2^2\rangle - 0.21\|1a_1^2 2a_1^2 1b_2^2\rangle - 0.21\|1a_1^2 3a_1^2 1b_2^2\rangle$
$14^1\Pi_g$	43.836 635	2.050	180.0	38.6	$\|14^1\Pi_g(^1B_2)\rangle \cong 0.74\|1a_1^2 3a_1^1 1b_2^2 2\bar{b}_2^1\rangle - 0.54\|1a_1^2 2a_1^1 1b_2^2 3\bar{b}_2^1\rangle$
$15^3\Pi_g$	43.836 303	2.047	180.0	38.8	$\|15^3\Pi_g(^3A_2)\rangle \cong 0.74\|1a_1^2 1b_1^1 1b_2^2 2b_2^1\rangle + 0.54\|1a_1^2 2a_1^1 1b_2^2 1a_2^1\rangle$
16^3B_1	43.835 733	1.932	180.0	39.2	$\|16^3B_1\rangle \cong 0.88\|1a_1^2 3a_1^1 1b_1^1 1b_2^2\rangle$
17^1B_2	43.835 717	2.338	49.1	39.2	$\|17^1B_2\rangle \cong 0.91\|1a_1^2 2a_1^2 3a_1^1 1\bar{b}_2^1\rangle$
$18^3B_{2,\,(global)}$	43.832 128	2.609	45.0	41.4	$\|18^3B_2\rangle \cong 0.66\|1a_1^2 2a_1^2 5a_1^1 1b_2^1\rangle - 0.57\|1a_1^2 2a_1^2 3a_1^1 1b_2^1\rangle$
$18^3B_{2,\,(local)}$	43.825 449	2.126	70.0	45.6	$\|18^3B_2\rangle \cong 0.63\|1a_1^2 2a_1^1 1b_2^2 2b_2^1\rangle - 0.50\|1a_1^2 2a_1^2 3a_1^1 1b_2^1\rangle$
19^3A_1	43.814 754	2.256	60.0	52.3	$\|19^3A_1\rangle \cong 0.69\|1a_1^2 2a_1^1 4a_1^1 1b_2^2\rangle - 0.50\|1a_1^2 2a_1^2 1b_2^1 2b_2^1\rangle$
20^3A_1	43.811 885	2.213	63.0	54.1	$\|20^3A_1\rangle \cong 0.75\|1a_1^2 2a_1^2 1b_2^1 2b_2^1\rangle$
21^5B_1	43.811 544	2.026	70.0	54.4	$\|21^5B_1\rangle \cong 0.94\|1a_1^2 2a_1^1 1b_1^1 1b_2^1 2b_2^1\rangle$
22^5A_2	43.809 653	2.153	55.5	55.5	$\|22^5A_2\rangle \cong 0.93\|1a_1^2 2a_1^1 4a_1^1 1b_1^1 1b_2^1\rangle$
23^1B_2	43.808 758	1.963	60.0	56.1	$\|23^1B_2\rangle \cong 0.89\|1a_1^2 2a_1^1 1b_1^2 1\bar{b}_2^1\rangle$
24^5A_1	43.806 526	2.090	72.6	57.5	$\|24^5A_1\rangle \cong 0.96\|1a_1^2 2a_1^1 3a_1^1 1b_2^1 2b_2^1\rangle$
25^5B_2	43.804 160	2.266	53.9	59.0	$\|25^5B_2\rangle \cong 0.96\|1a_1^2 2a_1^1 3a_1^1 4a_1^1 1b_2^1\rangle$
26^1A_2	43.800 618	2.058	58.0	61.2	$\|26^1A_2\rangle \cong 0.81\|1a_1^2 2a_1^1 3a_1^1 1\bar{b}_1^1 1\bar{b}_2^1\rangle$
27^3B_1	43.787 389	2.076	60.0	69.5	
$28^5\Pi_u$	43.787 296	2.097	180.0	69.6	$\|28^5\Pi_u(^5B_1)\rangle \cong 0.92\|1a_1^2 2a_1^1 1b_1^1 1b_2^1 2b_2^1\rangle$
29^3A_1	43.779 330	2.147	180.0	74.6	
$30^1\Pi_g$	43.758 164	2.202	180.0	87.8	
$31^5\Pi_g$	43.753 845	2.192	180.0	90.6	$\|31^5\Pi_g(^5A_2)\rangle \cong 0.70\|1a_1^1 2a_1^1 1b_1^1 1b_2^2 2b_2^1\rangle + 0.64\|1a_1^2 2a_1^1 1b_2^1 2b_2^1 1a_2^1\rangle$
32^7B_1	43.690 419	2.071	95.0	130.4	$\|32^7B_1\rangle \cong 0.98\|1a_1^1 2a_1^1 3a_1^1 1b_1^1 1b_2^1 2b_2^1\rangle$
33^7A_2	43.683 649	2.376	50.0	134.6	$\|33^7A_2\rangle \cong 0.98\|1a_1^1 2a_1^1 3a_1^1 4a_1^1 1b_1^1 1b_2^1\rangle$
34^7A_1	43.637 721	2.564	60.0	163.4	$\|34^7A_1\rangle \cong 0.99\|1a_1^1 2a_1^1 3a_1^1 5a_1^1 1b_2^1 2b_2^1\rangle$
35^7B_1	43.633 629	2.419	60.0	166.0	$\|35^7B_1\rangle \cong 0.88\|1a_1^1 2a_1^1 5a_1^1 1b_1^1 1b_2^1 2b_2^1\rangle + 0.34\|1a_1^1 2a_1^1 3a_1^1 1b_1^1 1b_2^1 2b_2^1\rangle$

another one from $1b_2$ to $1b_1$ while retaining the singly electrons highly coupled.

Slightly above there is a JT conical intersection that gives rise to two branches of $^1B_1$ ($|10^1B_1\rangle \cong 0.89|1a_1^2 2a_1^1 1\bar{b}_1^1 1b_2^2\rangle - 0.18|1a_1^2 2a_1^1 3a_1^2 1\bar{b}_1^1\rangle$) and $^1A_2$ ($|11^1A_2\rangle \cong 0.89|1a_1^2 2a_1^2 1b_1^1 1\bar{b}_2^1\rangle - 0.20|1a_1^2 3a_1^2 1b_1^1 1\bar{b}_2^1\rangle$) symmetry that relate to a $^1\Pi_u$ and $^1\Pi_g$ linear states, respectively, while they transform as $^1A''$ under C_s symmetry constraints (see Figure 2). By inspecting their equilibrium configurations we can see that these states are the singlet analogs of the 4 $^3B_1$ and 5 $^3A_2$ states, respectively (see above).

Another pair of JT-related states are the couple of 13 $^1A_1$ (with a minimum at 80.8° that relates to a $^1\Pi_u$ linear state) and 17 $^1B_2$ (with a minimum at 49.1° that relates to a $^1\Pi_g$ linear state) states that are the Renner − Teller companions of the above discussed 10 $^1B_1$ and 11 $^1A_2$ states, respectively.

Close enough there are two pairs of quintet spin symmetry states connected through a JT conical intersection.

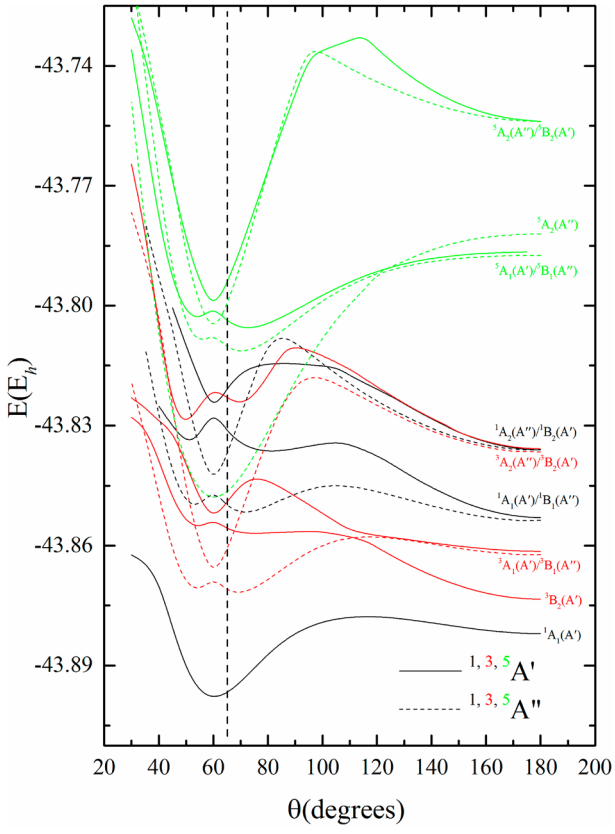

Figure 2. MRCI/aug − cc − pV5Z potential energy profiles of Be_3 states of singlet (black), triplet (red), and quintet (green) spin symmetry along the bending coordinate under C_s symmetry constraints.

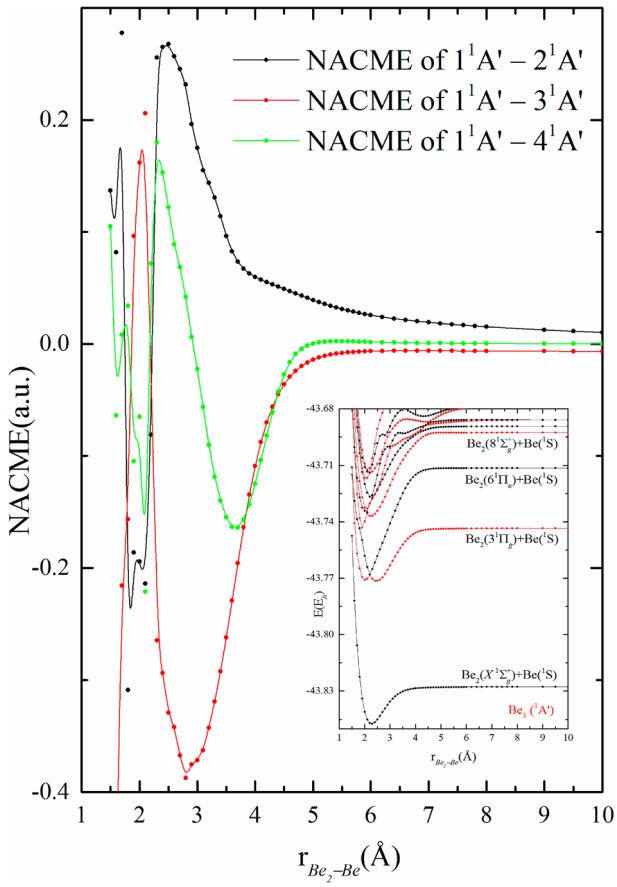

Figure 3. NACMEs at the SACASSCF/aug − cc − pV5Z computational level along the asymmetric (A′) dissociation path Be_3 (D_{3h}) → Be_2 + Be while retaining the Be_2 distance equal to the value of the ground state trimer. All states are of $^1A_1$ symmetry at their D_{3h} configuration.

The (energy) lowest pair splits off to a $21\,^5B_1$ ($|21\,^5B_1\rangle \cong 0.94|1a_1^2 2a_1^1 1b_1^1 1b_2^1 2b_2^1\rangle$) and a $22\,^5A_2$ ($|22\,^5A_2\rangle \cong 0.93|1a_1^2 2a_1^1 4a_1^1 1b_1^1 1b_2^1\rangle$) states. The other JT pair splits to $24\,^5A_1$ ($|24\,^5A_1\rangle \cong 0.96|1a_1^2 2a_1^1 3a_1^1 1b_2^1 2b_2^1\rangle$) and $25\,^5B_2$ ($|25\,^5B_2\rangle \cong 0.96|1a_1^2 2a_1^1 3a_1^1 4a_1^1 1b_2^1\rangle$) states. These four quintet states are interconnected at the Renner − Teller limit, *i.e.* $^5\Pi_u$ ($^5A_1$, $^5B_1$) and $^5\Pi_g$ ($^5A_2$, $^5B_2$).

The potential curves presented in both Figures 1 and 2 represent only a small fraction of all possible states of singlet, triplet, and quintet spin symmetry. We have only calculated the ground and the lowest two excited states of each space–spin symmetry. States of septet spin symmetry are also possible but they represent a chemical curiosity since all six valence electrons should be highly coupled. So, it is a surprise to us the existence of such a rich manifold of bound septet states. The energy lowest septet state has a very shallow minimum and it is of (32) $^7B_1$ ($|32\,^7B_1\rangle \cong 0.98|1a_1^1 2a_1^1 3a_1^1 1b_1^1 1b_2^1 2b_2^1\rangle$),$^7\Sigma_g^-$ at linearity symmetry. The deepest curve belongs to the 33 $^7A_2$ ($|33\,^7A_2\rangle \cong 0.98|1a_1^1 2a_1^1 3a_1^1 4a_1^1 1b_1^1 1b_2^1\rangle$) state that is the JT companion of the 32 $^7B_1$ one. In addition to the symmetry-imposed intersection at 60 degrees, the $^7A_2$ state suffers another intersection at around 75 degrees with a second $^7A_2$ state. With respect to the closed shell ground state a septet state results by fully uncoupling all its valence electrons.

4. Conclusions

We have studied at the highest possible level (MRCI/aug–cc − pV5Z) the Be_3 species. We report data on 35 states of singlet, triplet, quintet, and finally septet spin symmetry at both linear and bent configurations spanning an energy range of approximately160 kcal/mol. Its ground state is of closed shell character and results from the interaction of three excited ($2s^1 2p^1$) Be atoms. It is bound by *circa* 25 kcal/mol with respect to three Be (^1S) atoms. All other states result by exciting one, two, and/or three valence electrons to higher orbitals that either belong to the molecular plane or are perpendicular to it. This electron excitation breaks the $2c - 2e^-$ bond(s) of the ground state and the resulting asymmetry

is at the very heart of the JT distortion. A characteristic feature of the present work is the existence of septet spin states that result by fully uncoupling all six valence electrons. Their bound nature is due to the stabilisation of the kinetic energy within the molecular space provided.

Disclosure statement

No potential conflict of interest was reported by the author(s).

References

[1] R.E. Watson, Phys. Rev. **119**, 170 (1960). doi:10.1103/PhysRev.119.170

[2] A.W. Weiss, Phys. Rev. **122**, 1826 (1961). doi:10.1103/PhysRev.122.1826

[3] A. Kalemos, J. Chem. Phys. **145**, 214302 (2016). doi:10.1063/1.4967819

[4] A. Kalemos. Mol. Phys. **121**, e2230315 (2023). doi:10.1080/00268976.2023.2230315

[5] V.V. Meshkov, A.V. Stolyarov, M.C. Heaven, C. Haugen, and R.J. LeRoy, J. Chem. Phys. **140**, 064315 (2014). doi:10.1063/1.4864355

[6] N.N. Greenwood and A. Earnshaw, *Chemistry of the Elements* (Butterworth-Heinemann, Oxford, 1997).

[7] M. Bulski, Mol. Phys. **29**, 1171 (1975). doi:10.1080/00268977500100991

[8] R.J. Harrison and N.C. Handy, Chem. Phys. Lett. **123**, 321 (1986). doi:10.1016/0009-2614(86)80080-X

[9] T.J. Lee, A.P. Rendell and P.R. Taylor, J. Chem. Phys. **92**, 489 (1990). doi:10.1063/1.458570

[10] I.G. Kaplan, S. Roszak and J. Leszczynski, J. Chem. Phys. **113**, 6245 (2000). doi:10.1063/1.1287835

[11] J.M. Junquera-Hernández, J. Sánchez-Marín, G.L. Bendazzoli, and S. Evangelisti, J. Chem. Phys. **120**, 8405 (2014). doi:10.1063/1.1695328

[12] J.M. Junquera-Hernández, J. Sánchez-Marín, G.L. Bendazzoli, and S. Evangelisti, J. Chem. Phys. **121**, 7103 (2014). doi:10.1063/1.1792152

[13] J.I. Amaro-Estrada, A. Scemama, M. Caffarel, and A. Ramírez-Solís, J. Chem. Phys. **135**, 104311 (2011). doi:10.1063/1.3635403

[14] A. Ramírez-Solís and O. Novaro, Int. J. Quantum Chem. **112**, 2952 (2012). doi:10.1002/qua.24140

[15] M.C. Heaven, J.M. Merritt and V.E. Bondybey, Annu. Rev. Phys. Chem. **62**, 375 (2011). doi:10.1146/annurev-physchem-032210-102545

[16] M.M. Montero-Campillo, O. Mó, M. Yáñez, I. Alkorta, and J. Elguero, Adv. Inorg. Chem. **73**, 73 (2019). doi:10.1016/bs.adioch.2018.10.003

[17] N.B. Jaffe, J.F. Stanton and M.C. Heaven, J. Phys. Chem. Lett. **14**, 8339 (2023). doi:10.1021/acs.jpclett.3c02169

[18] A. Kalemos, J. Chem. Phys. **146**, 104307 (2017). doi:10.1063/1.4977930

[19] A. Kalemos, J. Phys. Chem. A. **122**, 8882 (2018). doi:10.1021/acs.jpca.8b07536

[20] A. Kalemos, Chem. Phys. Lett. **739**, 136964 (2020). doi:10.1016/j.cplett.2019.136964

[21] A. Kramida, Yu. Ralchenko, J. Reader, and NIST ASD Team (2022). *NIST Atomic Spectra Database* (ver. 5.10), [Online]. Available: https://physics.nist.gov/asd. National Institute of Standards and Technology, Gaithersburg, MD.

[22] T.H.Jr. Dunning, J. Chem. Phys. **90**, 1007 (1989). doi:10.1063/1.456153

[23] MOLPRO is a package of ab initio programs written by H.-J. Werner, P. J. Knowles, G. Knizia, F. R. Manby, M. Schütz, P. Celani, W. Györffy, D. Kats, T. Korona, R. Lindh, A. Mitrushenkov, G. Rauhut, K. R. Shamasundar, T. B. Adler, R. D. Amos, A. Bernhardsson, A. Berning, D. L. Cooper, M. J. O. Deegan, A. J. Dobbyn, F. Eckert, E. Goll, C. Hampel, A. Hesselmann, G. Hetzer, T. Hrenar, G. Jansen, C. Köppl, Y. Liu, A. W. Lloyd, R. A. Mata, A. J. May, S. J. McNicholas, W. Meyer, M. E. Mura, A. Nicklaß, D. P. O'Neill, P. Palmieri, D. Peng, K. Pflüger, R. Pitzer, M. Reiher, T. Shiozaki, H. Stoll, A. J. Stone, R. Tarroni, T. Thorsteinsson and M. Wang. MOLPRO, version 2012.1, a package of ab initio programs; University College Cardiff Consultants Limited: Cardiff, U.K., 2008.